Production of $X(3872)$ at high multiplicity

Eric Braaten,[*] Li-Ping He[,†] and Kevin Ingles[‡]

Department of Physics, The Ohio State University, Columbus, Ohio 43210, USA

Jun Jiang[§]

School of Physics, Shandong University, Jinan, Shandong 250100, China

The dependence of the production of the $X(3872)$ meson on the hadron multiplicity in pp collisions has been used as evidence against X being a charm-meson molecule. The argument is based in part on the incorrect assumption that the cross section for the breakup of X by scattering with comovers can be approximated by a geometric cross section inversely proportional to the binding energy of X. The breakup cross section should instead be approximated by the probability-weighted sum of the cross sections for the scattering of comoving pions from the charm-meson constituents of X, which is insensitive to the binding energy. A simple modification of the comover interaction model gives excellent fits to the data from the LHCb Collaboration on the multiplicity dependence of the production of X and $\psi(2S)$ using parameters compatible with X being a loosely bound charm-meson molecule.

I. INTRODUCTION

Since the unexpected discovery of the $X(3872)$ meson [also known as $\chi_{c1}(3872)$] in 2003 [1], dozens of other exotic heavy hadrons not predicted by the quark model have been discovered [2–5]. They present a major challenge to our understanding of QCD. The nature of $X(3872)$ (X for short) is a particularly important issue, because it remains the exotic heavy hadron for which the most detailed experimental information is available. The X was discovered in the decay mode $J/\psi\pi^+\pi^-$, and it has since been observed in six other decay modes. Its quantum numbers were determined in 2013 to be $J^{PC} = 1^{++}$ [6]. The LHCb Collaboration recently made the most precise measurements of its mass M_X and the first measurements of its decay width [7,8]. The difference between M_X and the $D^{*0}\bar{D}^0$ threshold is $\varepsilon_X = -0.07 \pm 0.12$ MeV. This implies an upper bound on the binding energy of X: $|\varepsilon_X| < 0.22$ MeV at 90% confidence level.

The information $J^{PC} = 1^{++}$ and $|\varepsilon_X| < 0.22$ MeV is sufficient to conclude that X must be a loosely bound S-wave molecule with the particle content $(D^{*0}\bar{D}^0 + D^0\bar{D}^{*0})/\sqrt{2}$

and with universal properties determined by ε_X [9]. The mean separation of its constituents is $r_X = (8\mu|\varepsilon_X|)^{-1/2}$, where μ is the reduced mass of $D^{*0}\bar{D}^0$. The upper bound $|\varepsilon_X| < 0.22$ MeV implies $r_X > 4.8$ fm. Thus, this amazing hadron has a radius more than an order of magnitude larger than that of ordinary hadrons. More relevant to the other exotic heavy hadrons is what X would have been if not for the fine-tuning of its mass to the $D^{*0}\bar{D}^0$ threshold. The possibilities that have been proposed include the P-wave charmonium state $\chi_{c1}(2P)$, an isospin-0 charm-meson molecule, and an isospin-1 compact tetraquark. In all these cases, the tuning of the mass to the $D^{*0}\bar{D}^0$ threshold produces resonant couplings to $D^{*0}\bar{D}^0$ and $D^0\bar{D}^{*0}$ that transforms X into a loosely bound molecule of neutral charm mesons.

Shortly after the discovery of X in B-meson decays [1], its existence was confirmed in $p\bar{p}$ collisions [10]. The production of X at a hadron collider can be resolved into two contributions: *prompt* production by strong interactions at the primary collision vertex and the *b-decay* contribution from weak decays of hadrons containing a bottom quark or antiquark at a displaced secondary vertex. The behavior of these two contributions may provide evidence for the nature of X. One significant difference is the hadronic environment in which X is embedded. In the decay of a b hadron, at most a few additional hadrons emerge from the secondary vertex. In prompt production at the LHC, hundreds of additional hadrons may emerge from the primary vertex. Collisions with comoving hadrons could break X up into its charm-meson constituents and thus decrease its prompt cross section.

[*]braaten.1@osu.edu
[†]he.1011@buckeyemail.osu.edu
[‡]ingles.27@buckeyemail.osu.edu
[§]jiangjun87@sdu.edu.cn

The LHCb Collaboration has studied the dependence on the hadron multiplicity of the production of X in pp collisions at the center-of-mass energy $\sqrt{s} = 8$ TeV [11]. The charmonium state $\psi(2S)$ (ψ' for short) provides a convenient benchmark, because it also decays into $J/\psi\pi^+\pi^-$, and its mass is close to M_X. The LHCb Collaboration measured the ratio of the prompt production rates for X and ψ' in the $J/\psi\pi^+\pi^-$ decay channel as functions of the number N_{tracks} of tracks in the vertex detector. The prompt X-to-ψ' ratio decreases significantly with increasing N_{tracks}.

Esposito *et al.* have used the comover interaction (CI) model to calculate the dependence of the prompt X-to-ψ' ratio on the charged-particle multiplicity N_{ch} [12]. Their result for X as a compact tetraquark is consistent with the LHCb data, while their result for X as a molecule with a geometric cross section decreases much too rapidly with N_{ch}. They concluded that the LHCb data support X being a tetraquark and strongly disfavor it being a molecule. Their results if X is a molecule were based in part on the incorrect assumption that its breakup reaction rate can be approximated by the geometric cross section πr_X^2, which is proportional to $1/|\varepsilon_X|$. It should instead be approximated by the cross section for scattering from the charm-meson constituents of X, which is insensitive to ε_X. We show below that a simple modification of the CI model provides excellent fits to the LHCb data on the multiplicity dependence of X and ψ' production with parameters compatible with X being a loosely bound charm-meson molecule.

II. COMOVER INTERACTION MODEL

The CI model was developed to describe the suppression of charmonium states in relativistic p-nucleus and nucleus-nucleus collisions by taking into account final-state interactions with comoving hadrons created by the collision [13–15]. Ferreiro used the CI model [16] to describe the suppression of ψ' relative to J/ψ in d-Au and p-Pb collisions at RHIC [17–19]. Ferreiro and Lansberg developed a more elaborate version of the CI model [20] to describe the suppression of $\Upsilon(2S)$ and $\Upsilon(3S)$ relative to Υ in p-Pb collisions at LHC [21,22]. A modified version of their model was applied by Esposito *et al.* to the production of X in pp collisions [12].

In the CI model, the survival probability of a $c\bar{c}$ or $b\bar{b}$ meson $\mathcal{Q}$ in pp collisions is [23]

$$S_{\mathcal{Q}} = \exp\left(-\frac{\langle v\sigma_{\mathcal{Q}}\rangle dN/dy}{\sigma_{pp}} \log\frac{dN/dy}{N_{pp}}\right), \quad (1)$$

where dN/dy is the light-hadron multiplicity per unit range of rapidity and $\langle v\sigma_{\mathcal{Q}}\rangle$ is the reaction rate for the breakup of $\mathcal{Q}$ averaged over comovers. The nondiffractive cross section $\sigma_{pp}(s)$ depends on the center-of-mass energy $\sqrt{s}$, while $N_{pp}(s, y)$ may also depend on the rapidity y. N_{pp} is the multiplicity below which the effects of comovers are

negligible: $S_{\mathcal{Q}} = 1$, if $dN/dy < N_{pp}$. The estimates for σ_{pp} in Ref. [12] are 63 mb at $\sqrt{s} = 7$ TeV and 70 mb at 13 TeV. A logarithmic interpolation in s gives $\sigma_{pp} = 65$ mb at $\sqrt{s} = 8$ TeV. The range of pseudorapidity for the LHCb spectrometer is $2.0 < \eta < 4.8$. An estimate of N_{pp} in that region can be obtained by multiplying the mean charged-particle multiplicity for the LHCb detector [24] by 3/2 to take into account neutral particles and then dividing by $\Delta y = 2.8$, which gives $N_{pp} \approx 6$.

In the CI model, the comovers are usually assumed to be either pions with mass $m_\pi \approx 140$ MeV or massless gluons. In Ref. [20], the momentum distribution of the comovers in the $\mathcal{Q}$ rest frame was assumed to be a Bose-Einstein distribution in the two-dimensional transverse plane with an effective temperature T_{eff}. In Ref. [12], it was assumed to be a three-dimensional Bose-Einstein distribution. Reference [20] introduced a simplistic model for the breakup cross section $\sigma_{\mathcal{Q}}$ as a function of the comover energy E_π: $\pi r_{\mathcal{Q}}^2(1 - E_{\mathcal{Q}}^{\text{thr}}/E_\pi)^n$, where $E_{\mathcal{Q}}^{\text{thr}}$ is the threshold energy for the breakup of $\mathcal{Q}$. In Ref. [12], that same model was used instead for the breakup reaction rate $v\sigma_{\mathcal{Q}}$. In Ref. [20], T_{eff} was determined by fitting data on the suppression of $\Upsilon(2S)$ and $\Upsilon(3S)$ in p-Pb and Pb-Pb collisions. The fitted value of T_{eff} is approximately linear in n between $\frac{1}{2}$ and 2, and its extrapolation to $n = 0$ is roughly 100 MeV. For $n = 1$, the effective temperature is $T_{\text{eff}} = (250 \pm 50)$ MeV. These same values of n and T_{eff} were used in Ref. [12].

III. ANALYSIS OF REF. [12]

In Ref. [12], their results for the prompt X-to-ψ' ratio were compared with preliminary LHCb data [25]. The theoretical results were normalized to the first LHCb data point at $N_{\text{tracks}} = 20$. As shown in Fig. 1, their narrow error
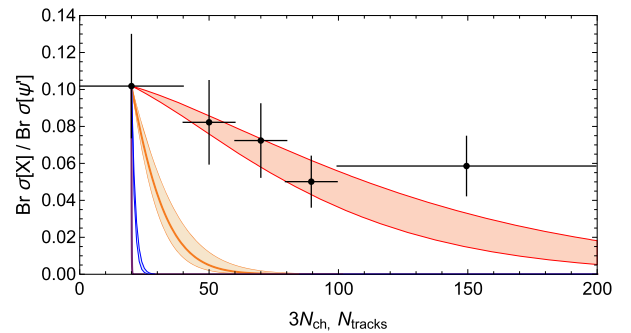

FIG. 1.   Prompt X-to-ψ' ratio as a function of the multiplicity N_{ch}. The preliminary LHCb data from Ref. [25] are shown in bins of N_{tracks}, which is identified with $3N_{\text{ch}}$. The two higher error bands are for a compact tetraquark from Ref. [12] (red band, near the data) and using their value of $\langle v\sigma_X\rangle$ (orange band). The two lower error bands are for a charm-meson molecule from Ref. [12] (blue band) and using their value of $\langle v\sigma_X\rangle$ (purple band, almost vertical).

band for a molecule decreases precipitously to almost 0 near $N_{\text{tracks}} = 25$, while their error band for a tetraquark gives a good fit to the LHCb data in the next three bins of N_{tracks}, which extend from 40 to 100.

It is implied in Ref. [12] that their error bands follow from inserting their breakup reaction rates $\langle v\sigma_Q \rangle$ into the ratio $S_X/S_{\psi'}$ of the survival probabilities given by Eq. (1). The values of $\langle v\sigma_Q \rangle$ in Ref. [12] are 5.15 ± 0.84 mb for ψ', 11.61 ± 1.69 mb for X if it is a tetraquark, and 1197 ± 171 mb for X if it is a molecule with $|\varepsilon_X| = 116$ keV. The prescription used to obtain these values was not specified. The resulting error bands are shown in Fig. 1. The error band using their value of $\langle v\sigma_X \rangle$ if X is a tetraquark decreases almost exponentially to 0, and it lies well below the LHCb data even in the second bin of N_{tracks}. Thus, the error bands in Ref. [12] must be determined by physics not captured by the survival probability in Eq. (1).

IV. πX BREAKUP REACTION RATES

Cross sections for low-energy πX scattering can be calculated using a nonrelativistic effective field theory for charm mesons and pions called XEFT [26]. It provides a systematically improvable description of the sector of QCD consisting of $D^*\bar{D}$, $D\bar{D}^*$, $D\bar{D}\pi$, or X with total energy near the $D^*\bar{D}$ threshold [26] and also the sector consisting of $D^*\bar{D}^*$, $D^*\bar{D}\pi$, $D\bar{D}^*\pi$, $D\bar{D}\pi\pi$, or $X\pi$ near the $D^*\bar{D}^*$ threshold [27]. A Galilean-invariant formulation of XEFT that exploits the approximate conservation of mass in the transitions $D^* \leftrightarrow D\pi$ was introduced in Ref. [28] and further developed in Ref. [29]. Galilean invariance guarantees that cross sections are the same in all Galilean frames, and it reduces the number of Feynman diagrams by requiring conservation of the total number of π, D^*, $\bar{D}^*$, and X mesons.

The breakup cross section for $\pi^+ X \to D^{*+}\bar{D}^{*0}$ was first calculated in Ref. [27] in the CM frame using original XEFT. The cross sections for $\pi^+ X \to D^{*+}\bar{D}^{*0}$ and $\pi^0 X \to D^{*0}\bar{D}^{*0}$ are calculated using Galilean-invariant XEFT in Ref. [30]. In Fig. 2, the cross sections are shown as functions of the collision energy E_c, which is the total kinetic energy in the CM frame. They have dramatic peaks near their thresholds, with peak values comparable to the geometric cross section πr_X^2, which is 1200 mb if $\varepsilon_X = 116$ keV. In the limit $\varepsilon_X \to 0$, the cross section for $\pi^+ X \to D^{*+}\bar{D}^{*0}$ approaches a delta function in E_c at $(\mu_{\pi X}/\mu_\pi)\delta_{0+}$, where $\delta_{0+} = 5.9$ MeV is the D^{*+}-to-$D^0\pi^+$ energy difference, and $\mu_{\pi X}$ and μ_π are the reduced masses for πX and πD. The energy-weighted integral of the P-wave contribution to the cross section reduces in the limit to

$$\int dE_c E_c \sigma[\pi^+ X \to D^{*+}\bar{D}^{*0}] \to \frac{2\pi\sqrt{2}\mu_{\pi X}^2 \delta_{0+}^{3/2} g^2}{\mu_\pi^{1/2}(2\sqrt{m_\pi}f_\pi)^2}, \quad (2)$$

where $g/(2\sqrt{m_\pi}f_\pi)$ is the D^{*0}-to-$D^0\pi^0$ coupling constant. This is the integral required to calculate the contribution to $\langle v\sigma_X \rangle$ from a three-dimensional Bose-Einstein distribution
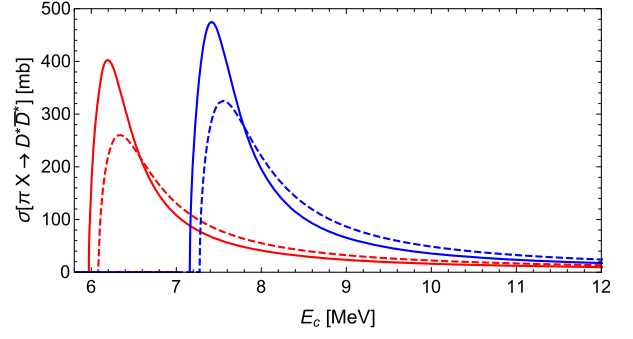

FIG. 2. Breakup cross sections for $\pi^+ X \to D^{*+}\bar{D}^0$ (red curves with lower threshold) and $\pi^0 X \to D^{*0}\bar{D}^0$ (blue curves with higher threshold) as functions of the collision energy. The binding energy of X is 116 keV (solid curves) and 232 keV (dashed curves).

of pions. The corresponding integral for $\pi^0 X \to D^{*0}\bar{D}^{*0}$ is obtained by replacing δ_{0+} by the D^{*0}-to-$D^0\pi^0$ energy difference $\delta_{00} = 7.0$ MeV. Their contribution to $\langle v\sigma_X \rangle$ decreases from 0.2 to 0.04 to 0.02 mb as T_{eff} increases from 100 to 200 to 300 MeV.

When the πX collision energy is well above the resonance region in Fig. 2, the pion can scatter off an individual constituent of X, and this will necessarily break up the bound state. The constituents of X are D^{*0} and $\bar{D}^0$ with probability $1/2$ and D^0 and $\bar{D}^{*0}$ with probability $1/2$. The total πX breakup cross section can be approximated by the weighted sum of πD and πD^* cross sections,

$$\sigma^{\text{incl}}[\pi X] \approx \frac{1}{2}(\sigma[\pi D^0] + \sigma[\pi\bar{D}^0] + \sigma[\pi D^{*0}] + \sigma[\pi\bar{D}^{*0}]). \quad (3)$$

A sufficient condition for the validity of this approximation is that E_c is well above the resonance region shown in Fig. 2.

For nonrelativistic collision energies, the largest cross sections are those allowed in Galilean-invariant XEFT. The specific final states from πX scattering taken into account by Eq. (3) are $D^*\bar{D}\pi$ and $D\bar{D}^*\pi$ with at least one neutral charm meson. The cross sections for $\pi D^0 \to \pi D$ and $\pi D^{*0} \to \pi D^*$ are calculated in Ref. [30]. In the region $\delta_{00} \ll E_c \ll m_\pi$, they are approximately constant. The total P-wave contribution to the πX breakup cross section using Eq. (3) is

$$\sigma^{\text{incl}}[\pi X] \approx \frac{4\mu_\pi^2(\mu_\pi^2 + \mu_{\pi*}^2)g^4}{\pi(2\sqrt{m_\pi}f_\pi)^4}, \quad (4)$$

where $\mu_{\pi*}$ is the πD^* reduced mass. An overestimate of the contribution of this region to $\langle v\sigma_X \rangle$ can be obtained by integrating over the range $\delta_{00} < E_c < m_\pi$. This estimate decreases from 0.05 to 0.02 to 0.01 mb as T_{eff} increases from 100 to 200 to 300 MeV.

For relativistic collision energies of order m_π and larger, XEFT is not applicable. There have been previous calculations of the reaction rates $\langle v\sigma \rangle$ for $\pi X \to D^* \bar{D}^*$ in a thermal gas of hadrons. In Ref. [31], the reaction rate decreases from 0.5 to 0.2 mb as the temperature T increases from 100 to 200 MeV. In Ref. [32], the reaction rate is approximately constant near 35 mb for T between 100 and 180 MeV. There have been previous calculations of the πD and πD^* reaction rates $\langle v\sigma \rangle$ in a thermal gas of hadrons. In Ref. [33], the πD and πD^* reaction rates from pion interactions were calculated at temperatures T from 116 to 156 MeV. The reaction rates are approximately independent of T, but they depend on a cutoff parameter Λ. As Λ increases from 0.5 to 1.0 to 1.5 GeV, the reaction rate from $\pi D \to \pi D$ increases from 2 to 6 to 10 mb. The reaction rate from $\pi D^* \to \pi D^*$ is much smaller, increasing from 0.007 to 0.04 to 0.1 mb. In Ref. [34], the structure of hadrons was taken into account by using a form factor with cutoff momentum Λ. For $\Lambda = \infty$, the estimate of $\langle v\sigma_X \rangle$ using Eq. (3) increases from 25 to 37 mb as T increases from 100 to 200 MeV, while for $\Lambda = 1$ GeV, $\langle v\sigma_X \rangle \approx 15$ mb almost independent of T.

V. ANALYSIS OF LHCB DATA

The LHCb data in Ref. [11] consist of the prompt fractions for both X and ψ' and the X-to-ψ' ratios for both prompt and b-decay production in Fig. 3. The horizontal bars attached to each data point indicate the bin of the variable N_{tracks}, and the value of N_{tracks} for the data point is at the multiplicity-weighted center of the bin. Since the pseudorapidity range of the LHCb vertex detector is $1.6 < \eta < 4.9$ [35], the multiplicity dN/dy can be approximated by $\frac{3}{2}(N_{\text{tracks}}/3.3)$. The prompt fraction f_{prompt} for ψ' is about 87% in the first bin of N_{tracks}. It first decreases as N_{tracks} increases, but then it appears to level off at about 70%. This behavior is incompatible with the assumption that the prompt cross section is proportional to the survival probability $S_{\psi'}$ given by Eq. (1). That assumption requires f_{prompt} to decrease almost exponentially to 0 as N_{tracks} increases.

A possible interpretation of the LHCb data on the prompt ψ' fraction in Fig. 3 is that the prompt cross section has two

components: one independent of dN/dy and the other proportional to $S_{\psi'}$. The two components could arise from the phase-space structure of the pp collisions. Prompt ψ''s created at a space-time point and with a momentum that puts them out of reach of most of the comoving pions give a contribution to the cross section that does not depend on dN/dy. The remaining prompt ψ''s are broken up with the probability $1 - S_{\psi'}$, so their contribution to the prompt cross section is proportional to $S_{\psi'}$.

This interpretation motivates a simple modification of the CI model. We denote the fraction of the prompt Q mesons out of reach of comoving pions by $f_{\text{out},Q}$ and their contribution to the prompt cross section by $\sigma_{\text{out},Q}$. The prompt cross section can be expressed as

$$\sigma_{\text{prompt}}[Q] = [1 + (1/f_{\text{out},Q} - 1)S_Q]\sigma_{\text{out},Q}, \quad (5)$$

which depends on dN/dy through S_Q. We assume the b-decay cross section $\sigma_{b\,\text{decay},Q}$ does not depend on dN/dy. The prompt fraction for Q is

$$f_{\text{prompt}}[Q] = \frac{1 + (1/f_{\text{out},Q} - 1)S_Q}{1 + 1/F_{\text{out},Q} + (1/f_{\text{out},Q} - 1)S_Q}, \quad (6)$$

where $F_{\text{out},Q} = \sigma_{\text{out},Q}/\sigma_{b\,\text{decay},Q}$. The prompt X-to-ψ' ratio is

$$\frac{\text{Br}\,\sigma_{\text{prompt}}[X]}{\text{Br}\,\sigma_{\text{prompt}}[\psi']} = N_{X/\psi'}\frac{1 + (1/f_{\text{out},X} - 1)S_X}{1 + (1/f_{\text{out},\psi'} - 1)S_{\psi'}}, \quad (7)$$

where $N_{X/\psi'}$ is the product of $\sigma_{\text{out},X}/\sigma_{\text{out},\psi'}$ and the ratio of the branching fractions into $J/\psi\pi^+\pi^-$. The b-decay X-to-ψ' ratio is

$$\frac{\text{Br}\,\sigma_{b\,\text{decay}}[X]}{\text{Br}\,\sigma_{b\,\text{decay}}[\psi']} = N_{X/\psi'}\frac{F_{\text{out},\psi'}}{F_{\text{out},X}}. \quad (8)$$

We have carried out a global fit to the LHCb data by minimizing the χ^2 for the 26 data points in Fig. 3 with respect to the five adjustable parameters in Eqs. (6)–(8) and
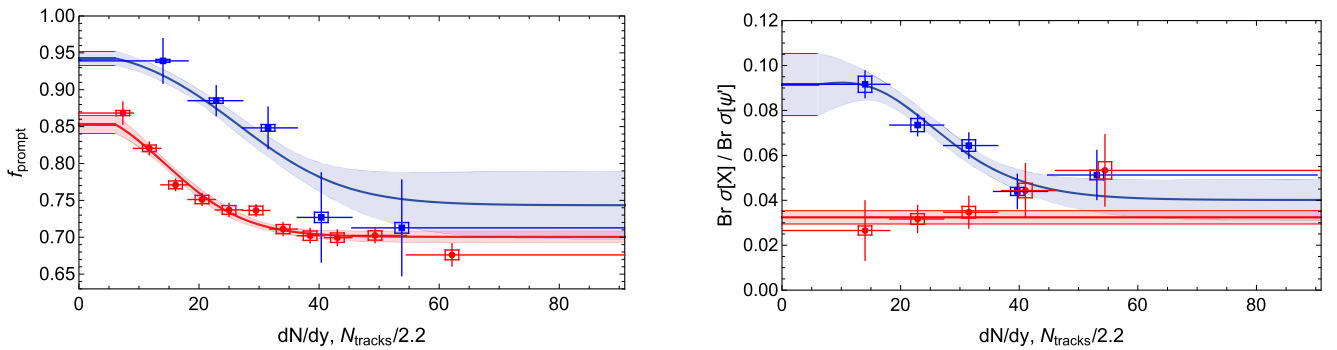

FIG. 3. Prompt fractions (left panel) and X-to-ψ' production ratios (right panel) as functions of the multiplicity dN/dy. The LHCb data in Ref. [11] for the prompt X fraction (blue squares), the prompt ψ' fraction (red dots), the prompt X-to-ψ' ratio (blue squares) and the b-decay X-to-ψ' ratio (red dots) are shown in bins of $N_{\text{tracks}}/2.2$. The curves and their error bands are from a global fit to the LHCb data.

the two breakup reaction rates $\langle v\sigma_X \rangle$ and $\langle v\sigma_{\psi'} \rangle$. Each data point is interpreted as the value at the multiplicity-weighted center of the bin, and its statistical and correlated errors are added in quadrature. The resulting fits are shown in Fig. 3. The error bands correspond to an increase of χ^2 by less than 1. The quality of the fits is very good with $\chi^2/\text{dof} = 0.99$. The fit to the b-decay X-to-ψ' ratio could be improved by adding a parameter that allows $\sigma_{\text{out},\psi'}$ or $\sigma_{b\,\text{decay},X}$ to increase linearly with dN/dy. The values of the seven fitted parameters are $f_{\text{out},\psi'} = 0.40 \pm 0.03$, $f_{\text{out},X} = 0.18 \pm 0.04$, $F_{\text{out},\psi'} = 2.3 \pm 0.1$, $F_{\text{out},X} = 2.9 \pm 0.7$, $\langle v\sigma_{\psi'} \rangle = 3.9 \pm 0.8\,\text{mb}$, $\langle v\sigma_X \rangle = 2.6 \pm 0.7$ mb, and $N_{X/\psi'} = 0.04 \pm 0.01$. The correlation matrix for these seven parameters is

$$
\begin{pmatrix}
1 & -0.40 & -0.59 & 0 & +0.83 & -0.28 & +0.35 \\
 & 1 & 0 & -0.22 & -0.45 & +0.86 & -0.86 \\
 & & 1 & -0.08 & -0.76 & 0 & +0.04 \\
 & & & 1 & 0 & -0.29 & -0.20 \\
 & & & & 1 & -0.40 & +0.43 \\
 & & & & & 1 & -0.83 \\
 & & & & & & 1
\end{pmatrix}.
$$

(9)

The fitted value of $\langle v\sigma_{\psi'} \rangle$ is about 1 σ smaller than the value in Ref. [12]. The fitted value of $\langle v\sigma_X \rangle$ is about 5 σ smaller than the value in Ref. [12] if X is a tetraquark. It is about 4 times larger than the contribution from $\pi X \rightarrow D^*\bar{D}^*$ in a thermal gas of hadrons with $T = 100$ MeV in Ref. [31]. The fitted value of $\langle v\sigma_X \rangle$ is less than $1/4$ the total breakup reaction rate from Ref. [34]. This could be attributed to a failure of the three-dimensional Bose-Einstein distribution as a model for comoving pions. A momentum distribution that is isotropic in the two transverse dimensions and the longitudinal dimension seems implausible.

VI. OUTLOOK

The LHCb data on the multiplicity dependence of the production of X and ψ' in pp collisions is incompatible with the assumption that the prompt cross section is proportional to the survival probability in Eq. (1). However, as shown in Fig. 3, a good global fit can be obtained by adding the assumption that some fraction $f_{\text{out},\mathcal{Q}}$ of the prompt $\mathcal{Q}$ cross section is out of reach of comoving pions. A microscopic description of pp collisions in which these fractions could be calculated would be useful.

The quantum numbers $J^{PC} = 1^{++}$ and the upper bound $|\varepsilon_X| < 0.22$ MeV imply that X must be a loosely bound S-wave molecule of neutral charm mesons with universal properties determined by ε_X. Universality is a double-edged sword. It allows definite statements about some properties of X, such as r_X and the πX breakup reaction rate, but it also makes them insensitive to what X would have been if not for the fine-tuning of its mass to the $D^{*0}\bar{D}^0$ threshold. X could have been a more compact charmonium or molecule or tetraquark, but it is transformed into a large neutral-charm-meson molecule by its resonant interactions with $D^{*0}\bar{D}^0$ and $D^0\bar{D}^{*0}$. Given the upper bound on $|\varepsilon_X|$, a model for X as a compact hadron should be interpreted as a fictitious hadron that does not couple to the charm mesons at the nearby $D^{*0}\bar{D}^0$ threshold. It may be an interesting exercise to rule out such a possibility using experimental data, but it is already excluded by theoretical considerations.

The universal physics of a loosely bound S-wave molecule reveals a dramatic failure of the simplistic model in Refs. [12] and [20] for $\langle v\sigma_{\mathcal{Q}} \rangle$ based on the geometric cross section $\pi r_{\mathcal{Q}}^2$. That model overestimates $\langle v\sigma_X \rangle$ by orders of magnitude. The breakup cross section σ_X is comparable to πr_X^2, which is proportional to $1/|\varepsilon_X|$, only at energies very close to the threshold as shown in Fig. 2. At higher energies, σ_X is determined by the cross sections for scattering from the constituents of X in Eq. (3), so $\langle v\sigma_X \rangle$ is insensitive to ε_X.

Our fit to the LHCb data in Fig. 3 may be a step towards a quantitative understanding of the production of X in high-energy hadron collisions. In a hadron collision, once X is broken up into charm mesons by the collision with a comoving pion, the probability that one of the charm mesons will encounter another charm meson and that they will coalesce into X is extremely small. An attempt to calculate the coalescence contribution to the production in pp collisions of X if it is a molecule was made in Ref. [12]. Coalescence can be much more important in p-nucleus and nucleus-nucleus collisions, because the number of charm meson that are created is much larger. The first observation of the production of X in heavy-ion collisions by the CMS Collaboration indicated that the prompt X-to-ψ' ratio may be much larger in Pb-Pb collisions than in pp collisions [36]. Understanding the production of X in p-nucleus and nucleus-nucleus collisions even at the qualitative level remains a challenging open problem.

[1] S. K. Choi *et al.* (Belle Collaboration), Observation of a Narrow Charmonium-Like State in Exclusive $B^{\pm} \to K^{\pm}\pi^{+}\pi^{-}J/\psi$ decays, Phys. Rev. Lett. **91,** 262001 (2003).

[2] A. Ali, J. S. Lange, and S. Stone, Exotics: Heavy pentaquarks and tetraquarks, Prog. Part. Nucl. Phys. **97,** 123 (2017).

[3] S. L. Olsen, T. Skwarnicki, and D. Zieminska, Nonstandard heavy mesons and baryons: Experimental evidence, Rev. Mod. Phys. **90,** 015003 (2018).

[4] M. Karliner, J. L. Rosner, and T. Skwarnicki, Multiquark States, Annu. Rev. Nucl. Part. Sci. **68,** 17 (2018).

[5] N. Brambilla, S. Eidelman, C. Hanhart, A. Nefediev, C. P. Shen, C. E. Thomas, A. Vairo, and C. Z. Yuan, The *XYZ* states: Experimental and theoretical status and perspectives, Phys. Rep. **873,** 1 (2020).

[6] R. Aaij *et al.* (LHCb Collaboration), Determination of the $X(3872)$ Meson Quantum Numbers, Phys. Rev. Lett. **110,** 222001 (2013).

[7] R. Aaij *et al.* (LHCb Collaboration), Study of the $\psi_2(3823)$ and $\chi_{c1}(3872)$ states in $B^+ \to (J\psi\pi^+\pi^-)K^+$ decays, J. High Energy Phys. 08 (2020) 123.

[8] R. Aaij *et al.* (LHCb Collaboration), Study of the lineshape of the $\chi_{c1}(3872)$ state, Phys. Rev. D **102,** 092005 (2020).

[9] E. Braaten and M. Kusunoki, Low-energy universality and the new charmonium resonance at 3870 MeV, Phys. Rev. D **69,** 074005 (2004).

[10] D. Acosta *et al.* (CDF Collaboration), Observation of the Narrow State $X(3872) \to J/\psi\pi^+\pi^-$ in $\bar{p}p$ Collisions at $\sqrt{s} = 1.96$ TeV, Phys. Rev. Lett. **93,** 072001 (2004).

[11] R. Aaij *et al.* (LHCb Collaboration), Observation of multiplicity-dependent prompt $\chi_{c1}(3872)$ and $\psi(2S)$ production in pp collisions, arXiv:2009.06619.

[12] A. Esposito, E. G. Ferreiro, A. Pilloni, A. D. Polosa, and C. A. Salgado, The nature of $X(3872)$ from high-multiplicity pp collisions, arXiv:2006.15044.

[13] A. Capella, A. Kaidalov, A. Kouider Akil, and C. Gerschel, J/ψ and ψ' suppression in heavy ion collisions, Phys. Lett. B **393,** 431 (1997).

[14] S. Gavin and R. Vogt, Charmonium Suppression by Comover Scattering in Pb + Pb Collisions, Phys. Rev. Lett. **78,** 1006 (1997).

[15] D. Kharzeev, C. Lourenco, M. Nardi, and H. Satz, A Quantitative analysis of charmonium suppression in nuclear collisions, Z. Phys. C **74,** 307 (1997).

[16] E. G. Ferreiro, Excited charmonium suppression in proton-nucleus collisions as a consequence of comovers, Phys. Lett. B **749,** 98 (2015).

[17] A. Adare *et al.* (PHENIX Collaboration), Nuclear Modification of ψ', χ_c, and J/ψ Production in d + Au Collisions at $\sqrt{s_{NN}} = 200$ GeV, Phys. Rev. Lett. **111,** 202301 (2013).

[18] B. B. Abelev *et al.* (ALICE Collaboration), Suppression of $\psi(2S)$ production in p-Pb collisions at $\sqrt{s_{NN}} = 5.02$ TeV, J. High Energy Phys. 12 (2014) 073.

[19] R. Arnaldi (ALICE Collaboration), Inclusive $\psi(2S)$ production in p-Pb collisions with ALICE, Nucl. Phys. **A931,** 628 (2014).

[20] E. G. Ferreiro and J. P. Lansberg, Is bottomonium suppression in proton-nucleus and nucleus-nucleus collisions at LHC energies due to the same effects?, J. High Energy Phys. 10 (2018) 094.

[21] S. Chatrchyan *et al.* (CMS Collaboration), Event activity dependence of $\Upsilon(nS)$ production in $\sqrt{s_{NN}} = 5.02$ TeV pPb and $\sqrt{s} = 2.76$ TeV pp collisions, J. High Energy Phys. 04 (2014) 103.

[22] M. Aaboud *et al.* (ATLAS Collaboration), Measurement of quarkonium production in proton–lead and proton–proton collisions at 5.02 TeV with the ATLAS detector, Eur. Phys. J. C **78,** 171 (2018).

[23] N. Armesto and A. Capella, A Quantitative reanalysis of J/ψ suppression in nuclear collisions, Phys. Lett. B **430,** 23 (1998).

[24] R. Aaij *et al.* (LHCb Collaboration), Measurement of charged particle multiplicities and densities in pp collisions at $\sqrt{s} = 7$ TeV in the forward region, Eur. Phys. J. C **74,** 2888 (2014).

[25] LHCb Collaboration, Multiplicity-dependent modification of $\chi_{c1}(3872)$ and $\psi(2S)$ production in pp collisions at $\sqrt{s} = 8$ TeV, CERN Report No. LHCb-CONF-2019-005, 2019.

[26] S. Fleming, M. Kusunoki, T. Mehen, and U. van Kolck, Pion interactions in the $X(3872)$, Phys. Rev. D **76,** 034006 (2007).

[27] E. Braaten, H. Hammer, and T. Mehen, Scattering of an ultrasoft pion and the $X(3872)$, Phys. Rev. D **82,** 034018 (2010).

[28] E. Braaten, Galilean-invariant effective field theory for the $X(3872)$, Phys. Rev. D **91,** 114007 (2015).

[29] E. Braaten, L.-P. He, and J. Jiang, Galilean-invariant effective field theory for the $X(3872)$ at next-to-leading order, Phys. Rev. D **103,** 036014 (2021).

[30] E. Braaten, L.-P. He, K. Ingles, and J. Jiang, Scattering of pions with $X(3872)$ (to be published).

[31] S. Cho and S. H. Lee, Hadronic effects on the X(3872) meson abundance in heavy ion collisions, Phys. Rev. C **88,** 054901 (2013).

[32] L. M. Abreu, K. P. Khemchandani, A. Martinez Torres, F. S. Navarra, and M. Nielsen, $X(3872)$ production and absorption in a hot hadron gas, Phys. Lett. B **761,** 303 (2016).

[33] J. Hong, S. Cho, T. Song, and S. H. Lee, Hadronic effects on the $cc\bar{q}\bar{q}$ tetraquark state in relativistic heavy ion collisions, Phys. Rev. C **98,** 014913 (2018).

[34] Z. w. Lin, T. G. Di, and C. M. Ko, Charm meson scattering cross-sections by pion and rho meson, Nucl. Phys. **A689,** 965 (2001).

[35] A. A. Alves, Jr. *et al.* (LHCb Collaboration), The LHCb detector at the LHC, J. Instrum. **3,** S08005 (2008).

[36] CMS Collaboration, Evidence for $\chi_{c1}(3872)$ in PbPb collisions and studies of its prompt production at $\sqrt{s_{NN}} = 5.02$ TeV, CERN Report No. CMS-PAS-HIN-19-005, 2019.s